

Orbitronics in Two-dimensional Materials

Tarik P. Cysne,^{1,*} Luis M. Canonico,² Marcio Costa,¹ R. B. Muniz,¹ and Tatiana G. Rappoport^{3,4,†}

¹*Instituto de Física, Universidade Federal Fluminense, 24210-346 Niterói RJ, Brazil*

²*Catalan Institute of Nanoscience and Nanotechnology (ICN2),*

CSIC and BIST, Campus UAB, Bellaterra, 08193 Barcelona, Spain

³*Physics Center of Minho and Porto Universities (CF-UM-UP), Campus of Gualtar, 4710-057, Braga, Portugal*

⁴*International Iberian Nanotechnology Laboratory (INL),*

Av. Mestre José Veiga, 4715-330 Braga, Portugal

(Dated:)

Orbitronics explores the control and manipulation of electronic orbital angular momentum in solid-state systems, opening new pathways for information processing and storage. One significant advantage of orbitronics over spintronics is that it does not rely on spin-orbit coupling, thereby broadening the range of non-magnetic materials that can be utilized for these applications. It also introduces new topological features related to electronic orbital angular momentum, and clarifies some long-standing challenges in understanding experiments that rely on the conventional concept of valley transport. This review highlights recent advances in orbitronics, particularly in relation to two-dimensional materials. We examine the fundamental principles underlying the generation, transport, and dynamics of orbital angular momentum to illustrate how the unique properties of two-dimensional materials can promote orbitronic phenomena. We also outline potential future research directions and address some outstanding questions in this field.

I. INTRODUCTION

The control of current flow by manipulating the spin degrees of freedom has led to the emergence of spintronics. Significant advances in this field over the past few decades [1–4] have provided innovative solutions to enhance the diversity, functionality, and efficiency of devices used for information processing and storage.

Spintronic phenomena in non-magnetic materials require the presence of spin-orbit coupling (SOC). This relativistic interaction, given by $\lambda \hat{\mathbf{S}} \cdot \hat{\mathbf{L}}$, couples the electronic spin operator $\hat{\mathbf{S}}$ with the orbital angular momentum (OAM) operator $\hat{\mathbf{L}}$. Its intensity λ is material dependent and increases rapidly with the atomic number Z of the constituent elements. A prominent spintronic phenomenon is the spin Hall effect (SHE), in which a transverse spin current is generated in response to a longitudinal applied electric field [5–7]. In addition to producing pure spin currents for practical applications in spintronic devices, the SHE may serve as a reliable identifier of the quantum spin Hall insulating phase. This topological phase of matter has spurred a considerable amount of research activity in condensed matter physics over the past two decades [8–10]. However, the need for a strong SOC may greatly limit the options for material selection. For instance, the relatively low atomic number of carbon presents a challenge to manipulating the electronic spin in pristine graphene. To address this limitation, one possible approach involves doping graphene with impurities that exhibit high spin-orbit coupling (SOC) values, or placing it sufficiently close to materials that can induce

SOC in graphene through the proximity effect, in order to improve its potential application in spintronics [4, 11]. Similar limitations occur in other materials composed of elements with low atomic numbers [12]. However, materials with naturally high SOC are relatively rare, and their extraction processes often incur significant environmental and economic costs [13].

It is worth noting that an electric field does not interact directly with the electronic spin but couples to the charge carriers and may affect their orbital angular momenta. This perturbation can propagate through the system, generating an OAM current that does not require the presence of SOC, and is not necessarily accompanied by a charge current. The use of electronic orbital angular momentum degrees of freedom for information processing and storage has given rise to the field of orbitronics, which has been evolving very rapidly in recent years.

Orbitronics shares similarities with spintronics. Several key spintronic effects, including the SHE, the inverse spin Hall effect (ISHE), the spin Rashba-Edelstein effect (SREE), and spin pumping, among others, have corresponding orbitronic analogs [14–16]. The ability to generate orbital angular momentum currents without relying on spin-orbit interaction significantly broadens the range of materials that can be employed in orbitronic applications. For example, the orbital Hall effect (OHE), which describes the emergence of a transverse orbital angular momentum current in response to a longitudinally applied electric field, was originally predicted to occur in p -doped silicon, a material characterized by weak spin-orbit coupling (SOC) [17]. For several years, few theoretical works explored the OHE foreseen by Bernevig, Hughes, and Zhang. Most of them focused on three-dimensional metallic materials [18–22], with a single exception that examined OHE in graphene [23]. Initially, some of the challenges in the field of orbitronics stemmed from ex-

* tarik.cysne@gmail.com

† tatiana.rappoport@inl.int

perimental difficulties in unambiguously identifying the accumulation and transport of OAM. On the theoretical side, the definition of OAM in periodic systems also presented significant hurdles [24–26]. For sometime, there was also a certain skepticism regarding the importance of orbital effects compared to spin effects. In part, because of a prevalent belief that OAM quenching would render orbital physics less significant. However, this perception has changed significantly in recent years due to theoretical and experimental advances in the field of orbitronics [27–30]. In fact, it took almost two decades, since its theoretical prediction, for the first direct observation of OHE to be announced in titanium [31]. Additional studies on other low-SOC materials followed [32, 33] and, more recently, OHE has also been reported in silicon [34], which was the material proposed in 2005 to exhibit this effect [17].

The OHE enables the generation of orbital angular momentum currents in non-magnetic systems, paving the way for the development of orbitronic devices. Conversely, inverse OHE can be utilized to detect these currents in certain materials. Other non-equilibrium orbitronic effects play a crucial role in manipulating electronic OAM. Notable examples include orbital torque (OT) effects [35–40] and orbital Rashba Edelstein effect (OREE) [41–44], also called orbital magnetoelectric effect. Along with their corresponding inverse phenomena linked to the Onsager reciprocity relations, they have introduced novel methods for manipulating orbital and spin angular momenta in nanostructures.

Although much of the research in orbitronics has focused on metallic three-dimensional systems, there is increasing interest in two-dimensional (2D) materials. The reduction in dimensionality significantly alters the crystalline field experienced by electrons in 2D materials compared to the bulk. This change affects orbital hybridizations, which can have a profound impact on orbital and electronic properties. For example, thin films of transition metal dichalcogenides (TMDs), with stoichiometry MX_2 , where M represents a transition metal atom and X denotes a chalcogen atom, exhibit electronic properties that depend on their composition, crystalline stacking, and thickness. Interestingly, these materials exhibit sizable orbital Hall conductivity plateaus within their semi-conducting gaps, where the spin Hall conductivity vanishes [45–47]. The H structural phase of MoS_2 is actually an orbital Hall insulator, characterized by an orbital Chern number C_{L_z} , which takes the value of one for the monolayer and two for the bilayer [48, 49]. Furthermore, TMD monolayers in their 2H and 1T structural phases have also been classified as higher-order topological insulators (HOTI) and they all display a plateau in orbital Hall conductivity within the band gap [47, 50, 51].

2D materials represent an exciting platform for research in orbitronics, particularly those of the van der Waals type. They can be exfoliated to produce ultrathin films down to monolayer thickness, which can be easily placed onto various substrates to create heterostructures

with unique orbitronic features [52–57].

This review highlights significant advances in the orbitronics of 2D materials. Section “Theoretical background”, provides an overview of some basic concepts underlying orbitronic effects. In Section “OAM in 2D Materials”, we discuss observations of orbital textures and some theoretical formulations of the orbital angular momentum operator, emphasizing their use in two-dimensional materials. Section “OHE in 2D Materials”, brings attention to progress related to the orbital Hall effect in two-dimensional materials. In Section “Controlling OAM”, we provide an overview of the current landscape of the orbital Rashba-Edelstein effect (OREE), and orbital torques (OT), as explored by researchers in the field of two-dimensional materials. Section “Effects of Disorder”, explores the consequences of disturbances caused by impurities and defects, with a particular emphasis on orbital relaxation processes and extrinsic contributions to the OHE and OREE. In the concluding section, we provide our insights into potential future research directions for orbitronics in 2D materials.

II. THEORETICAL BACKGROUND

Orbital Hall effect

The first proposal for the orbital Hall effect was presented by Bernevig *et al.* [17]. In their seminal work, they introduced it as an effect analogous to the spin Hall effect, but centered on the transport of OAM. Later, Go *et al.* in Ref. [28] proposed a microscopic mechanism that explains how OAM can be transported even in non-magnetic and centrosymmetric systems. In these systems, while *equilibrium* OAM is quenched, an external electric field induces a *non-equilibrium* OAM texture, leading to a transverse orbital current. Within linear response theory, the OHE can be mathematically expressed as:

$$\mathcal{J}_y^{L_z} = \sigma_{yx}^{L_z} \mathcal{E}_x, \quad (1)$$

where $\mathcal{J}_y^{L_z}$ represents the current density component along the \hat{y} direction of the OAM component L_z , induced by an electric field with intensity \mathcal{E}_x applied in the \hat{x} direction. The current density operator is defined by,

$$\hat{\mathbf{J}}^{L_z} = \frac{1}{2} \left(\hat{\mathbf{v}} \hat{L}_z + \hat{L}_z \hat{\mathbf{v}} \right), \quad (2)$$

where $\hat{\mathbf{v}}$ and \hat{L}_z represent the electronic velocity and z-component of the OAM operators, respectively.

For 2D systems, the orbital Hall conductivity (OHC) $\sigma_{yx}^{L_z}$ can be expressed as

$$\sigma_{yx}^{L_z} = e \sum_n \int_{\text{BZ}} \frac{d\mathbf{k}}{(2\pi)^2} f(\epsilon_n \mathbf{k}) \Omega_{yx,n}^{L_z}(\mathbf{k}), \quad (3)$$

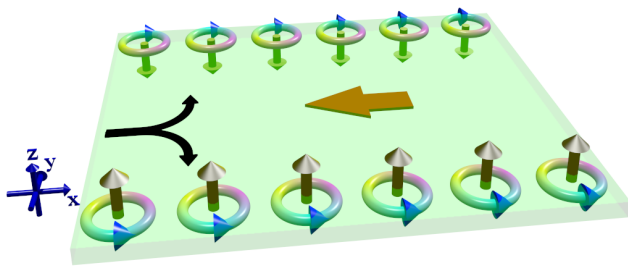


Figure 1. Schematic representation of orbital Hall Effect [Eq.(1)]. An electric current passing through the material induces a transverse flow of orbital angular momentum. The color gradient in the rings represents the phase gradient of electron wavefunctions, illustrating how electrons acquire orbital angular momentum and drift in opposite directions on either side of the material.

where the orbital Berry curvature is

$$\Omega_{yx,n}^{Lz}(\mathbf{k}) = 2\hbar \sum_{m \neq n} \text{Im} \left[\frac{\langle u_{n\mathbf{k}} | \hat{J}_{y,\mathbf{k}}^{Lz} | u_{m\mathbf{k}} \rangle \langle u_{m\mathbf{k}} | \hat{v}_x(\mathbf{k}) | u_{n\mathbf{k}} \rangle}{(\epsilon_{n\mathbf{k}} - \epsilon_{m\mathbf{k}} + i0^+)^2} \right]. \quad (4)$$

Here, the components $\alpha = x, y$ of the velocity operators may be obtained by $\hat{v}_\alpha(\mathbf{k}) = \hbar^{-1} \partial \hat{H}_{\mathbf{k}} / \partial k_\alpha$, $f(\epsilon)$ denotes the usual Fermi-Dirac distribution function and $|u_{n\mathbf{k}}\rangle$ is the cell-periodic part of the Bloch states with eigenvalue $\epsilon_{n\mathbf{k}}$.

Fig. 1 shows a schematic representation of the OHE and the resulting accumulation of OAM at the edges of a 2D system due to the transverse orbital current. This effect can occur in the absence of SOC as well as in the presence of spatial inversion and time-reversal symmetry. Within the picture of the mechanism introduced in Ref. [28], SOC partially transfers the transverse orbital current to the spin sector [$\sigma_{yx}^{Lz} \rightarrow \sigma_{yx}^{Sz}$], giving rise to SHE as a secondary phenomenon resulting from the more fundamental OHE.

The physical picture from Ref. [28] has greatly improved the understanding of OHE. However, it is worth noting that it relies on the intra-atomic approximation and may not provide a complete description compared to other formulations of the OAM operator, which will be discussed later. Additional contributions to this area are detailed in recent reviews focused on the broader aspects of orbitronics [14–16].

One may generalize the equation above to include other matrix elements of the orbital conductivity tensor $\sigma_{\mu,\nu}^{L\delta}$. This tensor obeys the same symmetry properties as the spin conductivity tensor [58, 59]. However, the physical picture elaborated in Ref. [28] applies to the elements of Eq. (1) and its cyclic permutations in the Cartesian indices x, y and z .

Orbital Rashba Edelstein effect

The OREE refers to the generation of orbital magnetization induced by an electric current. It is a Fermi-surface phenomenon that can occur in non-magnetic systems but requires the breaking of spatial-inversion symmetry [60]. The OREE can be regarded as the OAM analog of the well-known Rashba-Edelstein effect (REE), which is characteristic of systems without inversion symmetry and with strong SOC. Sometimes, the OREE is also called the kinetic magnetoelectric effect. A detailed clarification of the different terminologies used can be found in Ref. [61]. Unlike the OHE, the OREE has been observed and studied for a long time [62, 63] and was rediscovered by the orbitronics community. It can be described by the linear response formula

$$\mathcal{M}_\mu^L = \sum_\nu \alpha_{\mu\nu} \mathcal{E}_\nu, \quad (5)$$

where the non-equilibrium OAM density in μ -direction (\mathcal{M}_μ^L) generated by the electric field applied in the ν direction (\mathcal{E}_ν) is proportional to a matrix-element of the tensor $\alpha_{\mu\nu}$,

$$\alpha_{\mu\nu} = -e\tau_p \frac{\mu_B}{\hbar} \sum_n \int_{\text{BZ}} \frac{d\mathbf{k}}{(2\pi)^2} \left[\frac{\partial f}{\partial \epsilon} \right]_{\epsilon=E_F} \cdot \langle u_{n\mathbf{k}} | \hat{L}_\mu | u_{n\mathbf{k}} \rangle \langle u_{n\mathbf{k}} | \hat{v}_\nu(\mathbf{k}) | u_{n\mathbf{k}} \rangle, \quad (6)$$

where μ_B denotes the Bohr magneton. Eq. (6) is strongly constrained by crystal symmetry [64]. Since OREE is a Fermi surface effect, the previous equation can be expressed in terms of the charge current as follows:

$$\mathcal{M}_\mu^L = \sum_\nu \beta_{\mu\nu} \mathcal{J}_\nu, \quad (7)$$

where \mathcal{J}_ν is the charge current flowing in the ν -direction and $\beta_{\mu\nu} = \alpha_{\mu\nu} / \sigma_{\nu\nu}$, with $\sigma_{\nu\nu}$ being the longitudinal conductivity. Note that while the tensor $\alpha_{\mu\nu}$ is proportional to the momentum scattering time τ_p , the tensor $\beta_{\mu\nu}$ is independent of it [$\alpha_{\mu\nu} \propto \tau_p^1$ and $\beta_{\mu\nu} \propto \tau_p^0$]. Fig. 2 illustrates the OREE associated with the β_{zx} tensor component in Eq. 7.

There are 18 noncentrosymmetric point groups, known as gyrotropic groups, which allow finite matrix elements in the current-induced orbital magnetization tensor [64]: $C_1, C_2, C_3, C_4, C_6, C_{1v}, C_{2v}, C_{3v}, C_{4v}, C_{6v}, D_{2d}, S_4, D_2, D_3, D_4, D_6, T, O$. In addition, there are 3 noncentrosymmetric point groups, C_{3h}, D_{3h} , and T_d , that exhibit the necessary spatial inversion symmetry breaking but do not allow for current-induced magnetization [64]. The shape of the response tensor for each of the 18 gyrotropic point groups can be found in the literature [65]. Many subtleties of the microscopic mechanisms underlying the OREE, along with details on the various nomenclatures used in the literature, are discussed in a recent specialized review [42]. Here, we adopt a simple and intuitive explanation based on the

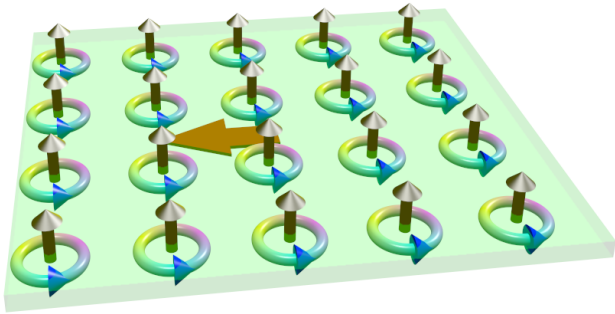


Figure 2. Schematic representation of orbital Rashba-Edelstein Effect [component β_{zx} of Eq.(7)]. An electric current passing through the material induces an orbital magnetization (golden arrows) oriented perpendicular to the current. The circulating electrons, driven by the phase gradient of their wavefunctions (color gradient in the rings), give rise to the orbital angular momentum.

Heisenberg equation of motion for the induced OAM in a solid subjected to an applied dynamical electric field [66]: $\frac{d\hat{\mathbf{L}}^{\text{Ind}}}{dt} = -\frac{i}{\hbar} [\hat{\mathbf{L}}^{\text{Ind}}, \hat{V}(t)] = \hat{\mathbf{r}} \times e\mathcal{E}(t)$, where $\hat{V}(t) = -e\mathcal{E}(t) \cdot \hat{\mathbf{r}}$ is a slowly switch-on electric potential. This general quantum mechanical equation indicates that the OREE arises from the torque applied to local electric dipoles within the solid: $\mathcal{M}^L \propto \mathbf{P} \times \mathcal{E}$ [54, 67].

Orbital torques

From a phenomenological point of view, the electric control of magnetization can be understood via the SOC, which acts together with the crystal field as a source of magnetic anisotropy -responsible for the orientation of the magnetization and orbital moments in ferromagnets [68, 69]. Consequently, a variation in the SOC can trigger magnetization dynamics due to the instantaneous change in the system's magnetic anisotropy. Given by $\mathcal{H}_{SOC} = \lambda(\mathbf{r})\hat{\mathbf{L}} \cdot \hat{\mathbf{S}}$, the SOC depends on three essential parameters: the electrostatic potential at the vicinity of the nucleus $\lambda(\mathbf{r})$, the spin $\hat{\mathbf{S}}$, and the OAM of the electrons $\hat{\mathbf{L}}$. Thus, changes in the SOC are given by

$$\begin{aligned} \delta\mathcal{H}_{SOC} &= \delta\lambda(\mathbf{r})\hat{\mathbf{L}} \cdot \hat{\mathbf{S}} + \lambda(\mathbf{r})\hat{\mathbf{L}} \cdot \delta\hat{\mathbf{S}} \\ &+ \lambda(\mathbf{r})\delta\hat{\mathbf{L}} \cdot \hat{\mathbf{S}}, \end{aligned} \quad (8)$$

where the first term in Eq. (8) encapsulates the variation of the atomic Coulomb potential due to the motion of the ions, the second term is related to changes in the spin density of the system, and the third term capture the changes in the OAM density. The first mechanism has been recently explored by Han *et al.* as a way of using the lattice to harvest spin and orbital moments [70]. The second channel connects directly to the spin-orbit torques [71], whereas the third describes the orbital torque in which a non-equilibrium orbital density triggers the magnetization dynamics. This mechanism was

proposed by Go and Lee in Ref. [35]. The system they used was a bilayer composed of a non-magnetic material (NM) and a ferromagnetic material (FM) with strong SOC. The NM material is formed by s - p hybridized orbitals (similar to the model used in Ref. [28]), while the FM is composed of d orbitals. The equilibrium magnetization \mathbf{M} of FM interacts with electronic spins density via exchange coupling $H_{xc}^{\text{FM}} = (J/\hbar) \mathbf{M} \cdot \hat{\mathbf{S}}$. The SOC of FM is given by $H_{so}^{\text{NM}} = (\alpha_{so}^{\text{FM}}/\hbar^2) \hat{\mathbf{L}} \cdot \hat{\mathbf{S}}$. When an electric field is applied, a transverse orbital current flows in the NM material due to the OHE. This orbital current is then transferred to the FM, injecting an OAM density, and the angular momentum of this nonequilibrium distribution is transferred to the spins via SOC. This process induces a torque in the magnetization of the FM material. The torque is given by

$$\mathbf{T} = \frac{J}{\hbar} \mathbf{M} \times \langle \hat{\mathbf{S}} \rangle^{\text{FM}}, \quad (9)$$

where $\langle \hat{\mathbf{S}} \rangle^{\text{FM}}$ is the spin accumulation produced in FM. Note that although the expression of Eq. (9) for OT depends on spin accumulation, it results from the injection of the OAM due to OHE in the NM material described by the third term in (8). This expression can be decomposed into field-like and damping-like components. While the field-like component arises from the intra-band term of linear response theory, the damping-like term is associated with inter-band contribution [35]. This phenomenon has been experimentally analyzed in various NM/FM bilayers and represents an important route for manipulating the OAM degree of freedom [72–74]. The reciprocal effect, orbital pumping, has been studied theoretically and its experimental evidence has also been reported [39, 70, 75–77].

Other orbital phenomena

The effects described in Eqs.(1-9), along with their reciprocal effects, can be viewed as building blocks for orbitronics devices within the generation-manipulation-detection paradigm, which is aimed at enabling efficient storage and processing of information using electronic OAM. Nevertheless, this has not exhausted the pool of orbitronic phenomena that could be useful for this task. Distinct mechanisms of orbital-charge conversion [78], and the interaction between OAM and pulsed light signals [79–81] are other topics currently under theoretical and experimental investigation. Here, we focused on the three building blocks, whose mechanisms and key references were outlined above.

III. ORBITAL ANGULAR MOMENTUM IN 2D MATERIALS

Orbital textures

The mechanism introduced in Ref. [28] to explain the OHE depends on the presence of orbital textures, \mathbf{k} -dependent orbital states, even in systems with inversion and time-reversal symmetry [82]. These textures, which describe the spatial distribution of orbital character, are an important feature in many 2D materials. Within the framework of the intra-atomic approximation (see the next subsection), these textures are associated with \mathbf{k} -dependent hopping processes involving different orbitals. However, 2D materials with broken inversion symmetry can give rise to OAM textures, described by $\ell_n(\mathbf{k}) = \langle u_{n\mathbf{k}} | \hat{\mathbf{L}} | u_{n\mathbf{k}} \rangle$, where $|u_{n\mathbf{k}}\rangle$ represents the periodic part of the Bloch wave functions. Such OAM textures highlight the unique role of symmetry breaking in 2D materials. They are found in various multi-orbital solids, including TMDs [45], bismuthene [46], and borophene [83].

Although the equilibrium OAM texture is quenched in non-magnetic and centrosymmetric systems, the presence of orbital textures can trigger a non-equilibrium OAM texture responsible for the occurrence of the OHE under the application of an electric field [28]. Experimental approaches based on analyzing angle-resolved photoemission spectroscopy signals have been developed to access the orbital and OAM textures of 2D materials and the surfaces of 3D materials [84, 85], applied to both equilibrium and non-equilibrium textures [84] and have been successfully used for in-depth studies of many compounds in the TMDs family [86, 87].

Multi-orbital v.s. single orbital materials

In the low-energy regime, carbon p_z orbitals are responsible for the electronic properties of graphene. This part of the Hilbert space, consisting of a single cubic harmonic state, does not support atomic OAM. Much of the discussion above is based on the intra-atomic approximation for the OAM operator, where the OAM of a solid is related to the OAM of individual atoms. This approach, also called the atom-centered approximation (ACA), becomes straightforward when the electronic Hamiltonian is expanded using a tight-binding basis, and it is commonly used in orbitronics. In graphene, the dominance of the p_z orbital causes the intra-atomic OAM to vanish, making orbitronic effects impossible under this approximation. A similar situation occurs in s -character band structures. However, electronic wave functions in solids are not always localized around atoms, and contributions to OAM from inter-site electron movement can be significant. This aspect has been explored in magnetic materials, where such contributions affect the *equilibrium* orbital magnetization. The *modern theory of orbital mag-*

netization [24, 25] has improved theoretical predictions for many magnetic systems and has a substantial impact on more exotic materials, significantly altering results compared to the intra-atomic approximation [88].

For isolated bands, Kohn demonstrated that Bloch electrons have an intrinsic orbital magnetic moment (OMM) [89]. Later, Chang and Niu reinterpreted this intrinsic OMM as the self-rotation of an electronic wave packet using a semi-classical approach [90]. Culcer et al. extended this concept by deriving a non-abelian (matrix) form of the OMM operator for nearly degenerate bands [91]. Pezo and coworkers further generalized the semi-classical expression of the OMM, incorporating matrix elements from the full Hilbert space [92]:

$$m_{n,m}^z(\mathbf{k}) = -i \frac{e}{2\hbar} \langle \vec{\nabla}_{\mathbf{k}} u_{n\mathbf{k}} | \times \left[\hat{H}_{\mathbf{k}} - \mathbb{1} \left(\frac{\epsilon_{n\mathbf{k}} + \epsilon_{m\mathbf{k}}}{2} \right) \right] | \vec{\nabla}_{\mathbf{k}} u_{m\mathbf{k}} \rangle, \quad (10)$$

where, $\vec{\nabla}_{\mathbf{k}} = \partial_{k_x} \vec{x} + \partial_{k_y} \vec{y}$, and $|u_{n(m)\mathbf{k}}\rangle$ is the periodic part of Bloch wave-function for the band with energy $\epsilon_{n(m)\mathbf{k}}$. Eq. (10) is analogous to the expression obtained from the semi-classical approach but is not restricted to the nearly degenerate subspace. The same expression was obtained by Ref. [93]. As pointed out in Ref. [94], an additional term must be added to Eq. (10) to ensure gauge invariance in the case of spatial energy bands. Recently, an additional quantum term has been predicted [95].

An OAM operator originating from this Bloch OMM can be defined [90, 96, 97]:

$$L_{n,m}^z(\mathbf{k}) = - \left(\frac{\hbar}{\mu_B g_L} \right) m_{n,m}^z(\mathbf{k}), \quad (11)$$

where, μ_B is the Bohr magneton and $g_L = 1$ is the Landé g -factor. This operator accounts for *both* intrasite and intersite contributions to OAM, going beyond the intra-atomic contribution [98].

The formulation of OHE based on Bloch OMM [97] has shown consistency with the intra-atomic approximation in predicting an orbital Hall insulating phase for bilayer of 2H-TMDs [49]. Nevertheless, the plateaus predicted by the intra-atomic approximation and the OMM approach have distinct heights and dependencies on the spectral energy band gap. Later, similar studies on other multi-orbital 2D materials were carried out [92]. Interestingly, even for single-orbital solids such as graphene [97] and s -orbital lattices [99], the formulation based on the OMM approach gives rise to a finite OHE. In these situations, the intra-atomic approximation yields a vanishing OHE, and all contributions must be attributed to the intersite movement of electrons. A pictorial representation of this movement was described in Ref. [99]. The OREE was also studied in 2D materials using the formulation of Bloch OMM [52, 53, 100, 101]. Studies on OT are often conducted using the intra-atomic approximation, which simplifies numerical calculations.

With the growing interest in comparing theoretical and experimental results, where disorder is an inherent feature of all materials, there is an increasing need for alternative formulations of the OAM operator in real space. One such approach is a basis-independent formulation using Green functions, expressed as:

$$\hat{L}_\gamma = -\varepsilon_{\alpha\beta\gamma} \frac{i\hbar^2}{4g_L\mu_B} \int dE \left[\text{Re}(G^+(\hat{H}, E)) \hat{v}_\alpha \delta(\hat{H} - E) \hat{v}_\beta + \hat{v}_\alpha \delta(\hat{H} - E) \hat{v}_\beta \text{Re}(G^-(\hat{H}, E)) \right], \quad (12)$$

that was introduced by Canonico *et al.* [102]. Within this approach, the off-diagonal elements of the position operator \mathbf{r} are computed from the perturbation theory

methods as $\langle i|r_\alpha|j\rangle = i\hbar \frac{\langle i|\hat{v}_\alpha|j\rangle}{E_j - E_i}$ ($\alpha = x, y, z$), where $|i\rangle$ and E_i are the i -th energy eigenstate of Hamiltonian \hat{H} with eigenvalue E_i . $G^-(\hat{H}, E)$ and $G^+(\hat{H}, E)$ are the advanced and retarded Green's functions respectively and $\varepsilon_{\alpha\beta\gamma}$ represent the Levi-Civita symbol. The formulation in Eq. (12) has been used to calculate the OHE due to the OMM in real space for disordered systems [102], where the expressions in Eqs. (10), (11) and (12) are used to describe the transport of OAM via the orbital current definition shown in Eq. (2).

The expression of Eq. 12 is inspired in the work of Bianco and Resta [26] that represents the macroscopic equilibrium orbital magnetization of a magnetic system as an integral of a local quantity and is equivalent to the more usual expression of the orbital magnetization, where the integration is performed in the reciprocal space:

$$\begin{aligned} M_z &= -\frac{e}{2\hbar c} \int \frac{d\mathbf{r}}{A} \text{Im} \langle \mathbf{r} | \hat{H} - \mu\mathbb{1} | [\mathbf{r}, \mathcal{P}] \times [\mathbf{r}, \mathcal{P}] | \mathbf{r} \rangle \\ &= -\frac{e}{2\hbar c} \text{Im} \sum_n \int_{\varepsilon_{n\mathbf{k}} \leq \mu} \frac{d\mathbf{k}}{(2\pi)^2} \langle \vec{\nabla}_{\mathbf{k}} u_{n\mathbf{k}} | \times (\hat{H}_{\mathbf{k}} + \mathbb{1}(\varepsilon_{n\mathbf{k}} - 2\mu)) | \vec{\nabla}_{\mathbf{k}} u_{n\mathbf{k}} \rangle. \end{aligned} \quad (13)$$

The first line of Eq. (13) represents the macroscopic orbital magnetization as an integral of a local quantity [24, 26]. A is the area of the sample, μ is the chemical potential, $\mathcal{P} = \sum_{\varepsilon_n < \mu} |\phi_n\rangle\langle\phi_n|$ is the projector over the occupied states, and $|\hat{H} - \mu\mathbb{1}| = (\hat{H} - \mu\mathbb{1})(\mathbb{1} - 2\mathcal{P})$ [103]. This expression exploits the spectral representation of the orbital moment due to its independence on the characteristics of the energy states and is suitable for computing the orbital moment in disordered materials. The second line in Eq. (13) in turn, is usual expression that exploits the periodicity of clean systems and represents it as a bulk property [24, 25], i.e., an integral of a geometric quantity over the BZ. Note that in both representations, the orbital magnetization does not depend on the explicit representation of the multi-orbital nature of the band structure. It depends only on the eigenstates and eigenvalues of the Hamiltonian of magnetic material.

IV. ORBITAL HALL EFFECT IN 2D MATERIALS

The reduced dimensionality and unique structural properties of 2D materials support the emergence of topological effects. Their planar structure also enables the control of the crystal field environment and manipulation of the symmetries governing the electronic properties. This has been extensively explored in spintronics research on 2D materials. For instance, reducing the symmetry group of a solid can lead to the emergence of novel components in the spin-conductivity tensor [58]. In

many 2D materials, this can be achieved and controlled through strain or proximity effects [104–108]. Similar behavior is expected in the OAM conductivity tensor [47], making these materials a flexible platform for investigating OAM transport properties. As a result, numerous studies have explored orbital transport in 2D materials [45–49, 67, 97, 99, 102, 109–128]. In this section, we highlight some of the most significant findings in this area, focusing on two key aspects in the orbitronics of 2D materials: the interplay between topological properties and OAM-related effects, and the reformulation of valleytronic concepts in light of the OHE.

Orbital topology

The quantum spin Hall insulator is a topological phase where the bulk has an energy band gap indexed by a \mathbb{Z}_2 topological invariant, which remains robust against smooth changes to the Hamiltonian. When the Fermi energy lies within this gap, linear response theory predicts a finite spin Hall conductivity, a hallmark of its non-trivial topology. Furthermore, creating boundaries in such systems reveals spin-polarized metallic edge states that carry the spin-Hall current, protected by time-reversal symmetry. This concept, introduced by Kane and Mele, is foundational in the study of topological insulators [9].

While these properties are well-established in the spin sector, analogous phenomena in the orbital sector have distinct differences. Refs. [45, 46] demonstrated that a finite OHC plateau can arise in certain insulating phases

of 2D systems (see Fig. 3b for the OHC of a MoS₂ bilayer). The p_x - p_y model on a honeycomb lattice, used to describe group-V materials grown on SiC substrates [129, 130], serves as an example [46]. In this model, the p_z orbital is excluded from the low-energy sector, leaving p_x and p_y orbitals to dominate electronic transport. Such orbital filtering provides an example of manipulating the OAM nature of a solid by altering the crystalline environment, a possibility widely explored in 2D materials.

Monolayers of TMDs with a 2H structural phase exhibit broken inversion symmetry, as can be seen in Fig. 3a if one considers only one layer. This leads to unique orbital-polarized edge states that cross the band-gap region when shaped into a nanoribbon with zigzag edges [54, 131], shown in Fig. 3c. These edge states are responsible for transporting the OHC [54]. Notably, monolayers of 2H-TMDs also display an OHC plateau within the insulating gap [45]. To further understand the origin of the OHC plateau and to differentiate it from effects purely related to inversion symmetry breaking, the OHC was calculated in bilayers of TMDs, which maintain inversion symmetry (see 3a) [48] and the plateau OHE persists. However, unlike the quantum spin Hall insulator, the orbital Hall insulator cannot be indexed by a \mathbb{Z}_2 topological invariant. Instead, the orbital Chern number, introduced in Refs. [48, 49], serves as a topological invariant for the orbital Hall insulating phase of 2H-TMDs. Monolayers of 2H-TMDs are characterized by an orbital Chern number $C_{L_z}^{11} = 1$, while bilayers have $C_{L_z}^{21} = 2$. In the low-energy regime, where the Hamiltonian can be written as Dirac-like Hamiltonian, the OHC plateau within the intra-atomic approximation is proportional to the orbital Chern number, $\sigma_{xy}^{L_z} = (\frac{e}{2\pi}) 2C_{L_z}$ [49]. The edge states in these systems, while related to the orbital Chern number, do not enjoy the same topological protection as those in the quantum spin Hall effect due to the absence of a \mathbb{Z}_2 invariant. Subsequent studies have further explored this topological invariant in other TMDs, showing their susceptibility to topological phase transitions [120, 121].

In Refs. [50, 51], it was proposed that monolayers of 2H-TMDs exhibit a higher-order topological insulator (HOTI) phase, characterized by the presence of corner states with fractional charge when the layer is fabricated in a flake geometry that preserves threefold rotational symmetry. These corner states manifest as discrete energy levels within the bulk band gap of the energy spectrum, indicating their topologically protected nature and distinguishing them from bulk or edge states (see Figure 3d). This higher-order topology is closely connected to the multi-orbital nature of 2H-TMDs. Subsequently, a study [47] linked this HOTI phase to a finite orbital Hall effect within the insulating gap in numerous TMD compounds that crystallize in two distinct structural phases: the non-centrosymmetric 2H phase and the centrosymmetric 1T phase. The connection between HOTI and OHE in these TMD phases was justified using symmetry arguments and supported by a study with an effective Bernevig-Hughes-Zhang (BHZ) toy model. Subsequent

works have extended the connections between topology and the multi-orbital nature of solids, particularly between HOTI and OHE [111, 132], in materials like 2D ferroelectrics and superconductors [133], as well as in 2D ferromagnets [127]. Additionally, well-established topological phenomena, such as the quantum Hall effect, are being reinterpreted with advances in understanding the orbital angular momentum (OAM) of electrons in solids [134].

Orbital v.s. valley transport

An appealing aspect of orbitronics in 2D materials is the often present multi-valley nature of their low-energy electronic structure. This implies that most of their electronic properties are governed by two inequivalent valleys, \mathbf{K} and \mathbf{K}' , in the Brillouin Zone (BZ). Such electronic structure is common in many 2D materials with honeycomb structure, such as graphene, hexagonal boron nitride, and 2H-TMDs, among others. The large separation between inequivalent valleys in the BZ suggested that they could be treated as well-defined quantum numbers, allowing them to store information [135]. Over the last two decades, this idea has been explored in a field known as valleytronics. However, as reviewed in Ref. [136], recent experimental and theoretical studies have revealed persistent inconsistencies with this idea despite all efforts at elucidation. In the standard valleytronic interpretation of typical experiments, an electric field applied to the material produces a transverse valley current via the valley Hall effect. Electrons with distinct valley quantum numbers accumulate at the sample edges. Opposite valley states are characterized by inverted OMM, which can be measured, for instance, using Kerr microscopy. In this view, the accumulation of OMM occurs as a secondary effect consequence of the valley Hall effect. This may seem contradictory because the valley quantum number, which serves as the principal transport quantity, is not directly measured. Instead, the accumulated OMM, typically considered a secondary consequence in valleytronics, can be assessed using Kerr microscopy. Additionally, the definition of valley current $\mathbf{J}_v = -e(\mathbf{v}|_{\mathbf{K}} - \mathbf{v}|_{\mathbf{K}'})$ depends on a valley filtering procedure that cannot be applied to Hamiltonians with strong inter-valley couplings [123]. Despite the challenges associated with this interpretation [136], it has been used to interpret many important experimental results [137–139].

In Ref. [97], Bowhal and Vignale argue that the concept of orbital current used in orbitronics could provide a more accurate description than the valley current approach previously utilized in valleytronics. Among other advantages, describing the system in terms of orbital current [using Eqs.(2) and (11)] highlights the OAM—a physical observable probed in experiments—as the primary quantity being transported. Interestingly, orbital and valley current obey distinct symmetry constraints. While the valley Hall effect requires the breaking of time-

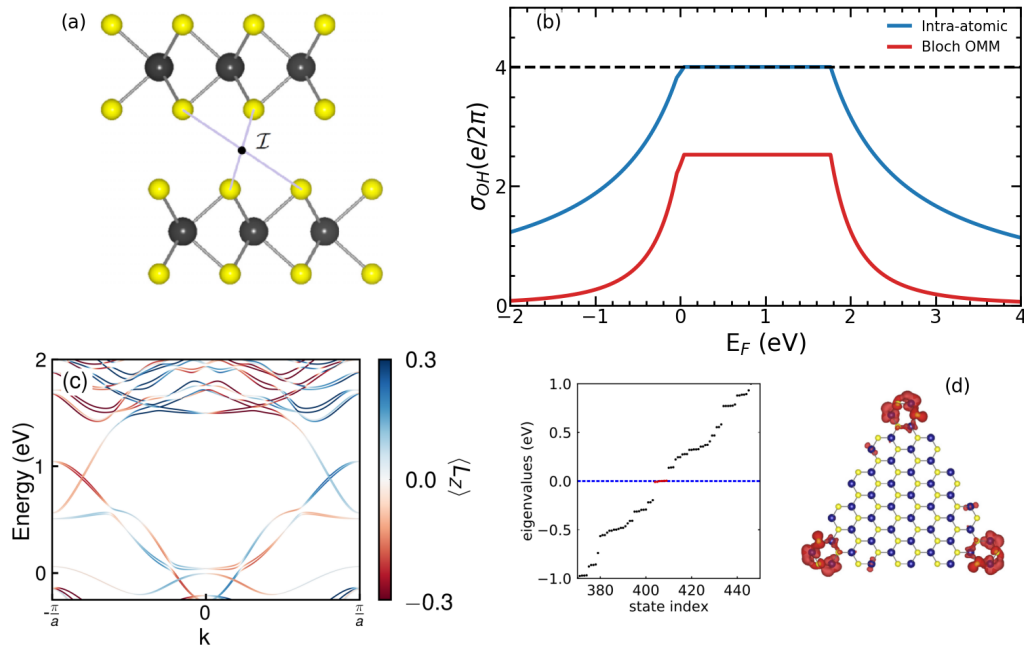


Figure 3. (a) Side view of a bilayer of 2H-TMD. \mathcal{I} represents the inversion-symmetry point. (b) The OHC plateau predicted by the low-energy theory for a bilayer of 2H-TMD. The blue curve represents the result obtained using the intra-atomic approximation, while the red curve represents the results derived from the Bloch OMM formulation. The dashed line marks the quantized value of the OHE plateau. (c) The energy spectrum of a MoS₂ nanoribbon with zigzag edges reveals OAM-polarized edge states that cross the bulk band and can transport OHC. (d) Energy spectra of triangular nanoflakes of MoS₂ with in-gap corner states and the corresponding image of the distribution probability associated with the corner-states wave function. Figures adapted from Refs. [47–49].

reversal or spatial inversion symmetry, the OHE does not have such a restriction [48, 49]. For this reason, the valleytronics community believed that centrosymmetric systems, such as the unbiased bilayer of 2H-TMDs, would not exhibit any transverse current response when a longitudinal electric field is applied. Nevertheless, it was later demonstrated that finite OHC could arise, and the resulting orbital accumulation might be detectable through Kerr rotation experiments [48, 49]. Even systems with strong inter-valley coupling, such as graphene with Kekulé distortions, can exhibit considerable OHE [123].

Recently, a study on h-BN/gapped graphene/h-BN moiré superlattice reported a strong correlation between theoretical calculations of OHC and non-local resistance measurements [117]. Additionally, a recent theoretical study [118] describing magnetoresistance due to Bloch OMM accumulation in bilayer systems found qualitative agreement with the experiment reported in Ref. [33], strengthening the idea of treating it as the primary quantity of transport. Finally, we mention that materials lacking a multivalley structure and SHE, but exhibiting significant OHC, are promising candidates for unambiguously probing orbitronic effects without interference from competing phenomena that might produce similar experimental signals. Phosphorene, a monolayer of black phosphorus, exemplifies such materials and also exhibits

highly anisotropic orbital transport properties [125].

V. CONTROLLING ORBITAL ANGULAR MOMENTUM IN 2D MATERIALS

Effects that allow the manipulation of the OAM degree of freedom, such as the orbital Rashba Edelstein effect (OREE), are closely related to the symmetries of solids [60, 65]. This has been widely studied in the context of spintronics in 2D materials [140, 141] and, as will become evident, offers opportunities to use these systems as platforms for precise OAM control. Additionally, the ability to fabricate heterostructures from different 2D materials can help designing efficient OT devices—a potentiality that has also been explored by the spintronics community of 2D materials [142, 143]. This section highlights advances in understanding the phenomena that enable OAM control in 2D materials.

Orbital Rashba Edelstein effect in 2D materials

In contrast to other orbitronic effects, OREE has been studied both theoretically and experimentally in 2D materials [52, 55, 144–146]. Many 2D materials belong to

the non-centrosymmetric D_{3h} point group, where the linear Edelstein effect is forbidden by symmetry [see discussion below Eq. (7)]. A crucial constraint in 2D materials for allowing OREE is that they can only have one mirror plane perpendicular to the plane of the material. This constraint helps explain why applying strain or cutting the system into a ribbon, thus introducing additional symmetry-breaking elements, can promote the appearance of the OREE. For instance, monolayers of 2H-TMDs, which belong to the D_{3h} point group, can exhibit a finite current-induced orbital magnetization when their three-fold rotational symmetry is broken through uniaxial strain. This reduces the crystal's point-group symmetry to C_{2v} and enables the OREE, as observed experimentally in Ref. [55] and discussed theoretically in Ref. [53]. Furthermore, fabricating 2D materials in a nanoribbon geometry can reduce their point-group symmetry without the need for a strain field, helping the onset of OREE.[54, 67].

Magnetic 2D materials, such as CrI_3 , exhibit broken time-reversal symmetry, and an equilibrium orbital magnetization may appear. Bilayers of these materials have the interesting properties of breaking time-reversal ($\mathcal{T} \rightarrow \times$) and spatial-inversion ($\mathcal{P} \rightarrow \times$) symmetries individually while preserving their combined operation ($\mathcal{P}\mathcal{T} \rightarrow \checkmark$). In this case, it is possible to modify the equilibrium orbital magnetization using an electric field without the flow of charge current; that is, a field-induced modification of orbital magnetization can be achieved [147]. This implies that even in an insulating state, the OAM can be controlled. This effect resembles the OREE but is governed by distinct symmetry properties [60] and a different microscopic mechanism. Along with the OREE, it belongs to the more general class of orbital magnetoelectric effects (see details on nomenclature in Ref. [61]). We note that current-induced orbital magnetization can arise even in higher-order terms in the electric field expansion. This phenomenon corresponds to the non-linear OREE [144, 148]. Experiments reporting this effect in 2D materials can already be found [145]. Such non-linear phenomena are often studied by the light-matter interaction community where orbitronics in 2D materials is also under investigation [122, 124, 128].

Torques and OAM in 2D materials

Orbital torque (OT) has been more extensively investigated in three-dimensional metallic material systems, with only a few studies explicitly addressing torques associated with electronic OAM in 2D materials. In 2D systems, relying solely on the OHE to generate OT is challenging because the OHE induces orbital accumulation at the edges of the plane. However, the orbital Rashba Edelstein effect provides a more effective mechanism by generating orbital magnetization throughout the entire plane. When a 2D magnetic layer is in contact with a material exhibiting OREE, this orbital magnetization

can exert torque on the magnetic layer, enabling OT.

Recent theoretical works have begun to explore OAM-related torque phenomena in 2D materials. Calculations by Atencia and co-workers [149] suggest the existence of an intrinsic torque on the OAM of Bloch electrons in the presence of an electric field, rooted in interband terms and related to the quantum metric tensor. This torque vanishes in two-band systems with particle-hole symmetric band structures but can be nonzero for tilted Dirac fermions. In Ref. [150], Canonico and co-workers report numerical calculations indicating a spin-orbit torque in the centrosymmetric 1T-TMD PtSe_2 , arising from the entanglement between spin and the OAM texture of electrons, which is distinct from conventional spin-orbit torques in non-centrosymmetric systems.

Although these studies are not directly related to the OT mechanism introduced in Ref. [35], they address phenomena rooted in electronic OAM that could be used for similar purposes. Given the significant impact of spin-torque phenomena on the spintronics community of 2D materials [151, 152] and the increasing sophistication in fabricating diverse van der Waals heterostructures, it is expected that research into OAM torque phenomena in 2D materials will expand in the coming years. These torque effects may play a crucial role in future applications within these advanced heterostructures [56, 57].

VI. EFFECTS OF DISORDER

Beyond idealized models, real-world applications of orbitronics require an understanding of the disorder, which is ubiquitous in the large-scale fabrication of any device. Building on the parallelism between spintronics and orbitronics, critical metrics for addressing the performance of orbitronic devices, such as the orbital diffusion lengths and the charge-to-orbital conversion, can be altered and even enhanced by the disorder. In the following, we separate the orbital relaxation and the extrinsic contributions to the orbital Hall effect and recollect recent experimental and theoretical work on these topics.

Orbital Relaxation and Orbital Dynamics

Following the direct experimental detection of the OHE through MOKE measurements, the experimental data raised additional inquiries about the orbital relaxation and the role of the disorder. Choi *et al.*, using MOKE and orbital torque measurements in Ti and Ti/FM systems, obtained orbital diffusion lengths of 74 ± 24 nm and 50 ± 15 nm [31], respectively, with the latter being in agreement with previous estimations on similar heterostructures [73]. In contrast, similar Moke measurements from Lyalin *et al.* in Cr reported orbital relaxation lengths of 6.6 ± 0.6 nm [32]. On the same order of magnitude, orbital Hanle measurements from Sala *et al.* in polycrystalline Mn suggested orbital relaxation

lengths of ~ 2 nm [33], which are in close agreement with the estimates from Liu *et al.* in CoPt/Cu/MgO heterostructures [153].

Though these experimental data seem to point out that disorder might be a limiting factor for orbital conductivity, there is experimental data that shows the contrary. Kim *et al.*, using orbital torque measurements, found orbital relaxation lengths in Cu samples that are about 10 nm, in agreement later the estimations from Kim *et al.* for CoFe/Cu/TiO₂ and CoFe/Cu/SiO₂ where the O from the oxide hybridizes with the Cu and consequently favors the orbital transport [154, 155]. Along the same lines, experiments from Seifert *et al.* suggested that ballistic orbital propagation occurs over 20 nm - in agreement with previous experiments from Hayashi *et al.* [73] - and little influence of the magnetic impurities on the orbital propagation [79]. Furthermore, recent experiments from Idrobo *et al.* analyzed the orbital relaxation in Ti-based devices and found orbital relaxation lengths of 7.9 nm with a strong dependence on sample morphology [156].

The differing estimates of orbital diffusion lengths suggest that orbital dynamics function differently from spin dynamics, offering a potential method to distinguish between spin and orbital signals. On the theoretical front, Han *et al.* investigated orbital dynamics in centrosymmetric systems. Combining symmetry arguments and quantum kinetic theory, they demonstrated the orbital and spin degrees of freedom have distinctive anticommutation relations that allow for orbital-momentum locking even in centrosymmetric systems. These couplings give rise to the orbital textures (different from OAM textures, as discussed above), contribute to the OAM dynamics, and, in nonequilibrium, give rise to the orbital Hall effect in metals [157].

Sohn *et al.* investigated the coupled spin-orbital dynamics in centrosymmetric materials using quantum kinetic theory and device simulations [158]. Their study demonstrated that orbital-momentum locking, arising from the orbital texture, leads to a Dyakonov-Perel-like orbital relaxation, suggesting that orbital angular momentum undergoes rapid decoherence. Conversely, Ref. 159 found a different behavior when studying the decay of orbital currents using first-principles quantum mechanical scattering calculations. By injecting orbital currents from an orbitally polarized lead into bulk transition metals, they observed that the orbital current persisted for only a few atomic layers, indicating a different relaxation mechanism than the one predicted in Ref. [158].

Recent calculations for a 2D tight-binding model using a quantum Boltzmann equation approach that takes into account different impurity models show that the impurity symmetry strongly influences the OAM relaxation that can change from Dyakonov-Perel-like to Elliot-Yafet relaxation if the axial symmetry of the impurity is broken [160].

Disorder effects and Extrinsic contributions to the OHE and OREE

Discrepancies in the estimates of orbital diffusion lengths also open the possibility for the influence of extrinsic contributions that may alter the orbital currents and OAM accumulation. Since the early days of spintronics, the effects of the disorder have been thoroughly studied and discussed [2]. Beyond influencing spin relaxation and decoherence, disorder can also give rise to the SHE through extrinsic mechanisms such as skew scattering and side-jump. These impurity-driven effects can generate spin currents even in materials where intrinsic mechanisms are weak or absent, demonstrating that disorder can play a fundamental role in spin transport phenomena.

In orbitronics, similar extrinsic mechanisms are expected to influence orbital transport, potentially generating OHE. Just as skew scattering and side-jump effects can drive SHE, these mechanisms are predicted to play a role in orbital dynamics by deflecting OAM currents in the presence of impurities. While the study of disorder-driven orbital transport is still in its early stages, recent works have begun to explore how extrinsic contributions affect OHE and orbital accumulation. Furthermore, the dichotomy between the atom-centered (intra-site) approximation and itinerant contributions (inter-site) for the orbital moment raises even more questions about the effects of the disorder on the orbital moment generation.

In the atomic centered approximation (ACA), the seminal paper from Bernevig *et al.* discusses the effect of disorder in p-doped semiconductors, where they argued that due to the symmetry of the system, the disorder effects enter as self-energy corrections in their linear response calculations due to the cancellation of the vertex corrections in the current operators [17]. Tanaka *et al.* demonstrated that for transition metals, the vertex correction considered within the first Born approximation has a negligible impact on the spin and orbital Hall conductivities [19]. Similar trends were obtained in recent work by Pezo *et al.* [116]. Recent work based on quantum Boltzmann equations suggests the existence of lattice symmetries where disorder might lead to vanishing orbital Hall currents [161]. Conversely, calculations for a 2D tight-binding model, a quantum Boltzmann equation approach with third order of perturbation theory shows the appearance of a sizable extrinsic contribution to the orbital Hall effect that depends on the impurity concentration n_i [160].

When it comes to the disorder effects on the OHE of itinerant orbital momentum, there is a set of recent theoretical results in 2D materials. Recent work from Liu *et al.* using quantum kinetic equations with the perturbative treatment of the disorder pointed out the appearance of extrinsic contributions that rapidly overcome the intrinsic contributions [153]. Subsequently, Canonico *et al.* developed a real-space numerical methodology capable of capturing disorder effects on the OHC nonperturbatively

[102]. Their calculations demonstrated that the trends obtained from the perturbation theory by Liu *et al.* and beyond the reach of perturbative treatments hinted that disorder can enhance the OHC from the ballistic up to the diffusive regime until the onset of localization where the orbital transport is reduced.

Further theoretical studies by Veneri *et al.*, using a nonperturbative descriptions of disorder in the dilute regime, found that the extrinsic contributions to the OHC are dominated by the skew-scattering mechanism. In this regime, the OHC is proportional to the inverse of the impurity concentration, meaning that as impurity concentration decreases, the skew-scattering effect becomes more significant, leading to an increase in OHC. These findings elucidate the origin of extrinsic contributions and emphasize the role of perturbation symmetries in shaping the extrinsic OHC [115]. A subsequent work performed a similar analysis but for centrosymmetric bilayer 2H-TMD [119].

Regarding the orbital Rashba Edelstein effect, the ACA formulation is almost unexplored. In contrast, the effects of the disorder on the itinerant orbital moments have been studied more extensively. In equilibrium calculations, within Keldysh Green's function formalism, Zhu *et al.* obtained a closed form for the equilibrium orbital moment for magnetic disordered systems [162]. While analyzing the magnetic 2DEG Rashba model, they found that white noise disorder does not affect the orbital moment, representing a shift in the redistribution of the orbital moment on energy due to the renormalization of the energy states caused by the disorder. Beyond this, Rou *et al.*, using semiclassical calculations, found that the charge-to-orbital conversion acquires two extrinsic contributions due to the weak disorder: skew-scattering and side-jump [163]. Although weak disorder can enhance charge-to-orbital conversion, due to its linear dependence on the scattering time, it can be rapidly disturbed in heavy disorder situations. Still, further investigation on the non-perturbative disordered regime in disordered 2D materials is required.

VII. FUTURE DIRECTIONS

The field of orbitronics in two-dimensional (2D) materials is currently experiencing a stimulating phase, with prospects of development along several lines. However, some challenges need to be addressed to fully realize its potential. One of them is the difficulty in disentangling the contributions of spin and orbital angular momentum

(OAM) to magnetic moment accumulations, especially in 2D materials with relatively strong spin-orbit interactions. Extracting these contributions requires the use of more refined experimental techniques, possibly involving optical probes. There is now direct evidence that OAM currents can be induced and flow through materials even with negligible spin-orbit interaction. Furthermore, these currents can also generate spin currents via spin-orbit coupling (SOC). Therefore, careful interpretation of the experimental results is required to accurately identify and quantify the contributions of OAM to spin-orbitronic processes.

Another promising line of investigation is exploring proximity effects to boost the capabilities of orbitronics. In spintronics, proximity effects have been successfully employed to induce spin-orbit coupling in graphene. Similarly, the close proximity of orbitronic materials to conductive materials can lead to new orbital hybridizations that may facilitate the transport of OAM currents across heterostructures. This approach could open up new possibilities for integrating orbitronics into existing 2D material platforms, enabling efficient OAM transport and expanding the scope of potential applications.

Identifying and engineering 2D materials capable of efficiently transporting OAM currents with minimal damping is critical. Relaxation of OAM poses a significant challenge for the practical implementation of orbitronic devices, as it limits the effective transmission distance of orbital information. Future research should focus on materials exhibiting inherently low OAM relaxation rates or explore strategies to mitigate relaxation through material design or external control. The inherent flexibility of 2D materials makes them particularly well suited for such design optimizations, providing a versatile platform for the development of advanced orbitronic technologies.

Exploring and optimizing orbital torque in 2D materials is also a promising area for future research. This often involves injecting orbital currents into other materials and therefore, understanding the mechanisms governing the transmission of orbital current across interfaces is of significant interest. The use of magnetic materials, as sources of OAM currents, is also very encouraging. They can generate OAM currents with unconventional polarizations, expanding the possibilities for spin-orbitronic applications [59].

The thin and flexible nature of 2D materials makes them ideal for developing compact, low-power devices, where efficient torque generation can enable advances in magnetic switching and data storage technologies.

-
- [1] A. Fert, Nobel lecture: Origin, development, and future of spintronics, *Rev. Mod. Phys.* **80**, 1517 (2008).
 - [2] J. Sinova, S. O. Valenzuela, J. Wunderlich, C. H. Back, and T. Jungwirth, Spin hall effects, *Rev. Mod. Phys.* **87**, 1213 (2015).
 - [3] E. C. Ahn, 2d materials for spintronic devices, *npj 2D Materials and Applications* **4**, 10.1038/s41699-020-0152-0 (2020).
 - [4] A. Avsar, H. Ochoa, F. Guinea, B. Özyilmaz, B. J. van Wees, and I. J. Vera-Marun, Colloquium: Spintronics

- in graphene and other two-dimensional materials, *Rev. Mod. Phys.* **92**, 021003 (2020).
- [5] M. Dyakonov and V. Perel, Current-induced spin orientation of electrons in semiconductors, *Physics Letters A* **35**, 459 (1971).
- [6] J. E. Hirsch, Spin hall effect, *Phys. Rev. Lett.* **83**, 1834 (1999).
- [7] J. Sinova, D. Culcer, Q. Niu, N. A. Sinitsyn, T. Jungwirth, and A. H. MacDonald, Universal intrinsic spin hall effect, *Phys. Rev. Lett.* **92**, 126603 (2004).
- [8] B. A. Bernevig and S.-C. Zhang, Quantum spin hall effect, *Phys. Rev. Lett.* **96**, 106802 (2006).
- [9] C. L. Kane and E. J. Mele, Quantum spin hall effect in graphene, *Phys. Rev. Lett.* **95**, 226801 (2005).
- [10] M. König, S. Wiedmann, C. Brüne, A. Roth, H. Buhmann, L. W. Molenkamp, X.-L. Qi, and S.-C. Zhang, Quantum spin hall insulator state in hgte quantum wells, *Science* **318**, 766 (2007), <https://www.science.org/doi/pdf/10.1126/science.1148047>.
- [11] W. Han, R. K. Kawakami, M. Gmitra, and J. Fabian, Graphene spintronics, *Nature Nanotechnology* **9**, 794–807 (2014).
- [12] R. Jansen, Silicon spintronics, *Nature Materials* **11**, 400–408 (2012).
- [13] T. G. Rappoport, First light on orbitronics as a viable alternative to electronics, *Nature* **619**, 38 (2023).
- [14] D. Go, D. Jo, H.-W. Lee, M. Kläui, and Y. Mokrousov, Orbitronics: Orbital currents in solids, *Europhysics Letters* **135**, 37001 (2021).
- [15] D. Jo, D. Go, G.-M. Choi, and H.-W. Lee, Spintronics meets orbitronics: Emergence of orbital angular momentum in solids, *npj Spintronics* **2**, 10.1038/s44306-024-00023-6 (2024).
- [16] P. Wang, F. Chen, Y. Yang, S. Hu, Y. Li, W. Wang, D. Zhang, and Y. Jiang, Orbitronics: Mechanisms, materials and devices, *Advanced Electronic Materials* 10.1002/aelm.202400554 (2024).
- [17] B. A. Bernevig, T. L. Hughes, and S.-C. Zhang, Orbitronics: The intrinsic orbital current in *p*-doped silicon, *Phys. Rev. Lett.* **95**, 066601 (2005).
- [18] H. Kontani, T. Tanaka, D. S. Hirashima, K. Yamada, and J. Inoue, Giant orbital hall effect in transition metals: Origin of large spin and anomalous hall effects, *Phys. Rev. Lett.* **102**, 016601 (2009).
- [19] T. Tanaka, H. Kontani, M. Naito, T. Naito, D. S. Hirashima, K. Yamada, and J. Inoue, Intrinsic spin hall effect and orbital hall effect in *4d* and *5d* transition metals, *Phys. Rev. B* **77**, 165117 (2008).
- [20] T. Tanaka and H. Kontani, Intrinsic spin and orbital hall effects in heavy-fermion systems, *Phys. Rev. B* **81**, 224401 (2010).
- [21] S. Zhang and Z. Yang, Intrinsic spin and orbital angular momentum hall effect, *Phys. Rev. Lett.* **94**, 066602 (2005).
- [22] H. Kontani, T. Tanaka, D. S. Hirashima, K. Yamada, and J. Inoue, Giant intrinsic spin and orbital hall effects in Sr_2MO_4 ($m = \text{Ru, Rh, Mo}$), *Phys. Rev. Lett.* **100**, 096601 (2008).
- [23] I. V. Tokatly, Orbital momentum hall effect in *p*-doped graphene, *Phys. Rev. B* **82**, 161404 (2010).
- [24] T. Thonhauser, D. Ceresoli, D. Vanderbilt, and R. Resta, Orbital magnetization in periodic insulators, *Phys. Rev. Lett.* **95**, 137205 (2005).
- [25] D. Xiao, J. Shi, and Q. Niu, Berry phase correction to electron density of states in solids, *Phys. Rev. Lett.* **95**, 137204 (2005).
- [26] R. Bianco and R. Resta, Orbital magnetization as a local property, *Phys. Rev. Lett.* **110**, 087202 (2013).
- [27] S. R. Park, C. H. Kim, J. Yu, J. H. Han, and C. Kim, Orbital-angular-momentum based origin of rashba-type surface band splitting, *Phys. Rev. Lett.* **107**, 156803 (2011).
- [28] D. Go, D. Jo, C. Kim, and H.-W. Lee, Intrinsic spin and orbital hall effects from orbital texture, *Phys. Rev. Lett.* **121**, 086602 (2018).
- [29] V. Sunko, H. Rosner, P. Kushwaha, S. Khim, F. Mazzola, L. Bawden, O. J. Clark, J. M. Riley, D. Kasinathan, M. W. Haverkort, T. K. Kim, M. Hoesch, J. Fujii, I. Vobornik, A. P. Mackenzie, and P. D. C. King, Maximal rashba-like spin splitting via kinetic-energy-coupled inversion-symmetry breaking, *Nature* **549**, 492–496 (2017).
- [30] S. R. Park, J. Han, C. Kim, Y. Y. Koh, C. Kim, H. Lee, H. J. Choi, J. H. Han, K. D. Lee, N. J. Hur, M. Arita, K. Shimada, H. Namatame, and M. Taniguchi, Chiral orbital-angular momentum in the surface states of Bi_2Se_3 , *Phys. Rev. Lett.* **108**, 046805 (2012).
- [31] Y.-G. Choi, D. Jo, K.-H. Ko, D. Go, K.-H. Kim, H. G. Park, C. Kim, B.-C. Min, G.-M. Choi, and H.-W. Lee, Observation of the orbital hall effect in a light metal ti, *Nature* **619**, 52–56 (2023).
- [32] I. Lyalin, S. Alikhah, M. Berritta, P. M. Oppeneer, and R. K. Kawakami, Magneto-optical detection of the orbital hall effect in chromium, *Phys. Rev. Lett.* **131**, 156702 (2023).
- [33] G. Sala, H. Wang, W. Legrand, and P. Gambardella, Orbital hantle magnetoresistance in a *3d* transition metal, *Phys. Rev. Lett.* **131**, 156703 (2023).
- [34] R. Matsumoto, R. Ohshima, Y. Ando, D. Go, Y. Mokrousov, and M. Shiraishi, *Observation of giant orbital hall effect in si* (2025), [arXiv:2501.14237 \[cond-mat.mtrl-sci\]](https://arxiv.org/abs/2501.14237).
- [35] D. Go and H.-W. Lee, Orbital torque: Torque generation by orbital current injection, *Phys. Rev. Res.* **2**, 013177 (2020).
- [36] D. Go, F. Freimuth, J.-P. Hanke, F. Xue, O. Gomonay, K.-J. Lee, S. Blügel, P. M. Haney, H.-W. Lee, and Y. Mokrousov, Theory of current-induced angular momentum transfer dynamics in spin-orbit coupled systems, *Phys. Rev. Res.* **2**, 033401 (2020).
- [37] A. Bose, F. Kammerbauer, R. Gupta, D. Go, Y. Mokrousov, G. Jakob, and M. Kläui, Detection of long-range orbital-hall torques, *Phys. Rev. B* **107**, 134423 (2023).
- [38] R. Fukunaga, S. Haku, H. Hayashi, and K. Ando, Orbital torque originating from orbital hall effect in zr, *Phys. Rev. Res.* **5**, 023054 (2023).
- [39] E. Santos, J. Abrão, D. Go, L. de Assis, Y. Mokrousov, J. Mendes, and A. Azevedo, Inverse orbital torque via spin-orbital intertwined states, *Phys. Rev. Appl.* **19**, 014069 (2023).
- [40] I. Lyalin and R. K. Kawakami, Interface transparency to orbital current, *Phys. Rev. B* **110**, 104418 (2024).
- [41] T. Yoda, T. Yokoyama, and S. Murakami, Orbital edelstein effect as a condensed-matter analog of solenoids, *Nano Letters* **18**, 916 (2018), pMID: 29373028, <https://doi.org/10.1021/acs.nanolett.7b04300>.
- [42] A. Johansson, Theory of spin and orbital edelstein ef-

- fects, *Journal of Physics: Condensed Matter* **36**, 423002 (2024).
- [43] S. A. Nikolaev, M. Chshiev, F. Ibrahim, S. Krishnia, N. Sebe, J.-M. George, V. Cros, H. Jaffrès, and A. Fert, Large chiral orbital texture and orbital edelstein effect in co/al heterostructure, *Nano Letters* **24**, 13465 (2024), pMID: 39433297, <https://doi.org/10.1021/acs.nanolett.4c01607>.
- [44] L. Chirulli, M. T. Mercaldo, C. Guarcello, F. Giazzotto, and M. Cuoco, Colossal orbital edelstein effect in noncentrosymmetric superconductors, *Phys. Rev. Lett.* **128**, 217703 (2022).
- [45] L. M. Canonico, T. P. Cysne, A. Molina-Sanchez, R. B. Muniz, and T. G. Rappoport, Orbital hall insulating phase in transition metal dichalcogenide monolayers, *Phys. Rev. B* **101**, 161409 (2020).
- [46] L. M. Canonico, T. P. Cysne, T. G. Rappoport, and R. B. Muniz, Two-dimensional orbital hall insulators, *Phys. Rev. B* **101**, 075429 (2020).
- [47] M. Costa, B. Focassio, L. M. Canonico, T. P. Cysne, G. R. Schleder, R. B. Muniz, A. Fazzio, and T. G. Rappoport, Connecting higher-order topology with the orbital hall effect in monolayers of transition metal dichalcogenides, *Phys. Rev. Lett.* **130**, 116204 (2023).
- [48] T. P. Cysne, M. Costa, L. M. Canonico, M. B. Nardelli, R. B. Muniz, and T. G. Rappoport, Disentangling orbital and valley hall effects in bilayers of transition metal dichalcogenides, *Phys. Rev. Lett.* **126**, 056601 (2021).
- [49] T. P. Cysne, S. Bhowal, G. Vignale, and T. G. Rappoport, Orbital hall effect in bilayer transition metal dichalcogenides: From the intra-atomic approximation to the bloch states orbital magnetic moment approach, *Phys. Rev. B* **105**, 195421 (2022).
- [50] J. Zeng, H. Liu, H. Jiang, Q.-F. Sun, and X. C. Xie, Multiorbital model reveals a second-order topological insulator in $1h$ transition metal dichalcogenides, *Phys. Rev. B* **104**, L161108 (2021).
- [51] S. Qian, G.-B. Liu, C.-C. Liu, and Y. Yao, C_n -symmetric higher-order topological crystalline insulators in atomically thin transition metal dichalcogenides, *Phys. Rev. B* **105**, 045417 (2022).
- [52] W.-Y. He, D. Goldhaber-Gordon, and K. T. Law, Giant orbital magnetoelectric effect and current-induced magnetization switching in twisted bilayer graphene, *Nature Communications* **11**, 10.1038/s41467-020-15473-9 (2020).
- [53] S. Bhowal and S. Satpathy, Orbital gyrotropic magnetoelectric effect and its strain engineering in monolayer NbX_2 , *Phys. Rev. B* **102**, 201403 (2020).
- [54] T. P. Cysne, F. S. M. Guimarães, L. M. Canonico, M. Costa, T. G. Rappoport, and R. B. Muniz, Orbital magnetoelectric effect in nanoribbons of transition metal dichalcogenides, *Phys. Rev. B* **107**, 115402 (2023).
- [55] J. Son, K.-H. Kim, Y. H. Ahn, H.-W. Lee, and J. Lee, Strain engineering of the berry curvature dipole and valley magnetization in monolayer mos_2 , *Phys. Rev. Lett.* **123**, 036806 (2019).
- [56] K. L. Seyler, D. Zhong, B. Huang, X. Linpeng, N. P. Wilson, T. Taniguchi, K. Watanabe, W. Yao, D. Xiao, M. A. McGuire, K.-M. C. Fu, and X. Xu, Valley manipulation by optically tuning the magnetic proximity effect in wse_2/cr_3 heterostructures, *Nano Letters* **18**, 3823 (2018), pMID: 29756784, <https://doi.org/10.1021/acs.nanolett.8b01105>.
- [57] D. Zhong, K. L. Seyler, X. Linpeng, R. Cheng, N. Sivadas, B. Huang, E. Schmidgall, T. Taniguchi, K. Watanabe, M. A. McGuire, W. Yao, D. Xiao, K.-M. C. Fu, and X. Xu, Van der waals engineering of ferromagnetic semiconductor heterostructures for spin and valleytronics, *Science Advances* **3**, e1603113 (2017), <https://www.science.org/doi/pdf/10.1126/sciadv.1603113>.
- [58] A. Roy, M. H. D. Guimarães, and J. Sławińska, Unconventional spin hall effects in nonmagnetic solids, *Phys. Rev. Mater.* **6**, 045004 (2022).
- [59] M. Seemann, D. Ködderitzsch, S. Wimmer, and H. Ebert, Symmetry-imposed shape of linear response tensors, *Phys. Rev. B* **92**, 155138 (2015).
- [60] S. Hayami, M. Yatsushiro, Y. Yanagi, and H. Kusunose, Classification of atomic-scale multipoles under crystallographic point groups and application to linear response tensors, *Phys. Rev. B* **98**, 165110 (2018).
- [61] K. Osumi, T. Zhang, and S. Murakami, Kinetic magnetoelectric effect in topological insulators, *Communications Physics* **4**, 10.1038/s42005-021-00702-4 (2021).
- [62] E. L. Ivchenko and G. E. Pikus, New photogalvanic effect in gyrotropic crystals, *ZhETF Pisma Redaktsiiu* **27**, 640 (1978).
- [63] L. E. Vorob'ev, E. L. Ivchenko, G. E. Pikus, I. I. Farbshtein, V. A. Shalygin, and A. V. Shturbin, Optical activity in tellurium induced by a current, *Soviet Journal of Experimental and Theoretical Physics Letters* **29**, 441 (1979).
- [64] T. Furukawa, Y. Watanabe, N. Ogasawara, K. Kobayashi, and T. Itou, Current-induced magnetization caused by crystal chirality in nonmagnetic elemental tellurium, *Phys. Rev. Res.* **3**, 023111 (2021).
- [65] W.-Y. He and K. T. Law, Magnetoelectric effects in gyrotropic superconductors, *Phys. Rev. Res.* **2**, 012073 (2020).
- [66] L. Salemi, M. Berritta, A. K. Nandy, and P. M. Oppeneer, Orbitaly dominated rashba-edelstein effect in noncentrosymmetric antiferromagnets, *Nature Communications* **10**, 10.1038/s41467-019-13367-z (2019).
- [67] T. P. Cysne, F. S. M. Guimarães, L. M. Canonico, T. G. Rappoport, and R. B. Muniz, Orbital magnetoelectric effect in zigzag nanoribbons of p -band systems, *Phys. Rev. B* **104**, 165403 (2021).
- [68] P. Bruno, Tight-binding approach to the orbital magnetic moment and magnetocrystalline anisotropy of transition-metal monolayers, *Phys. Rev. B* **39**, 865 (1989).
- [69] J. M. D. Coey and S. S. Parkin, *Handbook of Magnetism and Magnetic Materials* (Springer Cham, 2021).
- [70] S. Han, H.-W. Ko, J. H. Oh, H.-W. Lee, K.-J. Lee, and K.-W. Kim, Orbital pumping incorporating both orbital angular momentum and position, *Phys. Rev. Lett.* **134**, 036305 (2025).
- [71] A. Manchon, J. Železný, I. M. Miron, T. Jungwirth, J. Sinova, A. Thiaville, K. Garello, and P. Gambardella, Current-induced spin-orbit torques in ferromagnetic and antiferromagnetic systems, *Rev. Mod. Phys.* **91**, 035004 (2019).
- [72] D. Lee, D. Go, H.-J. Park, W. Jeong, H.-W. Ko, D. Yun, D. Jo, S. Lee, G. Go, J. H. Oh, K.-J. Kim, B.-G. Park, B.-C. Min, H. C. Koo, H.-W. Lee, O. Lee, and K.-J. Lee, Orbital torque in magnetic bilayers, *Nature Communications* **12**, 10.1038/s41467-021-26650-9 (2021).

- [73] H. Hayashi, D. Jo, D. Go, T. Gao, S. Haku, Y. Mokrousov, H.-W. Lee, and K. Ando, Observation of long-range orbital transport and giant orbital torque, *Communications Physics* **6**, [10.1038/s42005-023-01139-7](https://doi.org/10.1038/s42005-023-01139-7) (2023).
- [74] Y. Yang, P. Wang, J. Chen, D. Zhang, C. Pan, S. Hu, T. Wang, W. Yue, C. Chen, W. Jiang, L. Zhu, X. Qiu, Y. Yao, Y. Li, W. Wang, and Y. Jiang, Orbital torque switching in perpendicularly magnetized materials, *Nature Communications* **15**, [10.1038/s41467-024-52824-2](https://doi.org/10.1038/s41467-024-52824-2) (2024).
- [75] H. Hayashi, D. Go, S. Haku, Y. Mokrousov, and K. Ando, Observation of orbital pumping, *Nature Electronics* **7**, 646–652 (2024).
- [76] D. Go, K. Ando, A. Pezo, S. Blügel, A. Manchon, and Y. Mokrousov, Orbital pumping by magnetization dynamics in ferromagnets, arXiv preprint arXiv:2309.14817 (2023).
- [77] J. E. Abrão, E. Santos, J. L. Costa, J. G. S. Santos, J. B. S. Mendes, and A. Azevedo, Anomalous spin and orbital hall phenomena in antiferromagnetic systems, *Phys. Rev. Lett.* **134**, 026702 (2025).
- [78] E. Santos, J. E. Abrão, A. S. Vieira, J. B. S. Mendes, R. L. Rodríguez-Suárez, and A. Azevedo, Exploring orbital-charge conversion mediated by interfaces with CuO_x through spin-orbital pumping, *Phys. Rev. B* **109**, 014420 (2024).
- [79] T. S. Seifert, D. Go, H. Hayashi, R. Rouze-gar, F. Freimuth, K. Ando, Y. Mokrousov, and T. Kampfrath, Time-domain observation of ballistic orbital-angular-momentum currents with giant relaxation length in tungsten, *Nature Nanotechnology* **18**, 1132 (2023).
- [80] P. Wang, Z. Feng, Y. Yang, D. Zhang, Q. Liu, Z. Xu, Z. Jia, Y. Wu, G. Yu, X. Xu, and Y. Jiang, Inverse orbital hall effect and orbitronic terahertz emission observed in the materials with weak spin-orbit coupling, *npj Quantum Materials* **8**, [10.1038/s41535-023-00559-6](https://doi.org/10.1038/s41535-023-00559-6) (2023).
- [81] Y. Xu, F. Zhang, A. Fert, H.-Y. Jaffres, Y. Liu, R. Xu, Y. Jiang, H. Cheng, and W. Zhao, Orbitronics: light-induced orbital currents in ni studied by terahertz emission experiments, *Nature Communications* **15**, [10.1038/s41467-024-46405-6](https://doi.org/10.1038/s41467-024-46405-6) (2024).
- [82] S. Han, H.-W. Lee, and K.-W. Kim, Microscopic study of orbital textures, *Current Applied Physics* **50**, 13–24 (2023).
- [83] F. Crasto de Lima, G. J. Ferreira, and R. H. Miwa, Orbital pseudospin-momentum locking in two-dimensional chiral borophene, *Nano Letters* **19**, 6564 (2019), pMID: 31424949, <https://doi.org/10.1021/acs.nanolett.9b02802>.
- [84] S. Beaulieu, J. Schusser, S. Dong, M. Schüler, T. Pincelli, M. Dendzik, J. Maklar, A. Neef, H. Ebert, K. Hricovini, M. Wolf, J. Braun, L. Rettig, J. Minár, and R. Ernstorfer, Revealing hidden orbital pseudospin texture with time-reversal dichroism in photoelectron angular distributions, *Phys. Rev. Lett.* **125**, 216404 (2020).
- [85] F. Mazzola, W. Brzezicki, M. T. Mercaldo, A. Guarino, C. Bigi, J. A. Miwa, D. De Fazio, A. Crepaldi, J. Fujii, G. Rossi, P. Orgiani, S. K. Chaluvadi, S. P. Chalil, G. Panaccione, A. Jana, V. Polewczyk, I. Vobornik, C. Kim, F. Miletto-Granozio, R. Fittipaldi, C. Ortix, M. Cuoco, and A. Vecchione, Signatures of a surface spin-orbital chiral metal, *Nature* **626**, 752–758 (2024).
- [86] S. Beaulieu, M. Schüler, J. Schusser, S. Dong, T. Pincelli, J. Maklar, A. Neef, F. Reinert, M. Wolf, L. Rettig, J. Minár, and R. Ernstorfer, Unveiling the orbital texture of $1t\text{-tite}_2$ using intrinsic linear dichroism in multi-dimensional photoemission spectroscopy, *npj Quantum Materials* **6**, [10.1038/s41535-021-00398-3](https://doi.org/10.1038/s41535-021-00398-3) (2021).
- [87] M. Schüler and S. Beaulieu, Probing topological floquet states in wse_2 using circular dichroism in time- and angle-resolved photoemission spectroscopy, *Communications Physics* **5**, [10.1038/s42005-022-00944-w](https://doi.org/10.1038/s42005-022-00944-w) (2022).
- [88] J.-P. Hanke, F. Freimuth, A. K. Nandy, H. Zhang, S. Blügel, and Y. Mokrousov, Role of berry phase theory for describing orbital magnetism: From magnetic heterostructures to topological orbital ferromagnets, *Phys. Rev. B* **94**, 121114 (2016).
- [89] W. Kohn, Theory of bloch electrons in a magnetic field: The effective hamiltonian, *Phys. Rev.* **115**, 1460 (1959).
- [90] M.-C. Chang and Q. Niu, Berry phase, hyperorbits, and the hofstadter spectrum: Semiclassical dynamics in magnetic bloch bands, *Phys. Rev. B* **53**, 7010 (1996).
- [91] D. Culcer, Y. Yao, and Q. Niu, Coherent wave-packet evolution in coupled bands, *Phys. Rev. B* **72**, 085110 (2005).
- [92] A. Pezo, D. García Ovalle, and A. Manchon, Orbital hall effect in crystals: Interatomic versus intra-atomic contributions, *Phys. Rev. B* **106**, 104414 (2022).
- [93] B. Göbel, L. Schimpf, and I. Mertig, Topological orbital hall effect caused by skyrmions and antiferromagnetic skyrmions, *Communications Physics* **8**, [10.1038/s42005-024-01925-x](https://doi.org/10.1038/s42005-024-01925-x) (2025).
- [94] Óscar Pozo Ocaña and I. Souza, Multipole theory of optical spatial dispersion in crystals, *SciPost Phys.* **14**, 118 (2023).
- [95] H. Liu, J. H. Cullen, D. P. Arovas, and D. Culcer, Quantum correction to the orbital hall effect, *Phys. Rev. Lett.* **134**, 036304 (2025).
- [96] M.-C. Chang and Q. Niu, Berry curvature, orbital moment, and effective quantum theory of electrons in electromagnetic fields, *Journal of Physics: Condensed Matter* **20**, 193202 (2008).
- [97] S. Bhowal and G. Vignale, Orbital hall effect as an alternative to valley hall effect in gapped graphene, *Phys. Rev. B* **103**, 195309 (2021).
- [98] I. Souza and D. Vanderbilt, Dichroic f -sum rule and the orbital magnetization of crystals, *Phys. Rev. B* **77**, 054438 (2008).
- [99] O. Busch, I. Mertig, and B. Göbel, Orbital hall effect and orbital edge states caused by s electrons, *Phys. Rev. Res.* **5**, 043052 (2023).
- [100] L.-k. Shi and J. C. W. Song, Symmetry, spin-texture, and tunable quantum geometry in a wte_2 monolayer, *Phys. Rev. B* **99**, 035403 (2019).
- [101] J. M. Lee, M. J. Park, and H.-W. Lee, Orbital edelstein effect of electronic itinerant orbital motion at edges, *Phys. Rev. B* **110**, 134436 (2024).
- [102] L. M. Canonico, J. H. Garcia, and S. Roche, Orbital hall responses in disordered topological materials, *Phys. Rev. B* **110**, L140201 (2024).
- [103] W. Andreoni and S. Yip, *Handbook of materials modeling* (Springer, 2020).
- [104] C. K. Safeer, N. Ontoso, J. Ingla-Aynés, F. Herling, V. T. Pham, A. Kurzman, K. Ensslin,

- A. Chuvilin, I. Robredo, M. G. Vergniory, F. de Juan, L. E. Hueso, M. R. Calvo, and F. Casanova, Large multidirectional spin-to-charge conversion in low-symmetry semimetal *MoTe₂* at room temperature, *Nano Letters* **19**, 8758 (2019), pMID: 31661967, <https://doi.org/10.1021/acs.nanolett.9b03485>.
- [105] C. K. Safeer, J. Ingla-Aynés, F. Herling, J. H. Garcia, M. Vila, N. Ontoso, M. R. Calvo, S. Roche, L. E. Hueso, and F. Casanova, Room-temperature spin hall effect in graphene/mo₂ van der waals heterostructures, *Nano Letters* **19**, 1074 (2019), <https://doi.org/10.1021/acs.nanolett.8b04368>.
- [106] L. Camosi, J. Světlík, M. V. Costache, W. Saverio Torres, I. Fernández Aguirre, V. Marinova, D. Dimitrov, M. Gospodinov, J. F. Sierra, and S. O. Valenzuela, Resolving spin currents and spin densities generated by charge-spin interconversion in systems with reduced crystal symmetry, *2D Materials* **9**, 035014 (2022).
- [107] M. Vila, C.-H. Hsu, J. H. Garcia, L. A. Benítez, X. Waintal, S. O. Valenzuela, V. M. Pereira, and S. Roche, Low-symmetry topological materials for large charge-to-spin interconversion: The case of transition metal dichalcogenide monolayers, *Phys. Rev. Res.* **3**, 043230 (2021).
- [108] T. P. Cysne, A. Ferreira, and T. G. Rappoport, Crystal-field effects in graphene with interface-induced spin-orbit coupling, *Phys. Rev. B* **98**, 045407 (2018).
- [109] V. o. T. Phong, Z. Addison, S. Ahn, H. Min, R. Agarwal, and E. J. Mele, Optically controlled orbitronics on a triangular lattice, *Phys. Rev. Lett.* **123**, 236403 (2019).
- [110] M. Zeer, D. Go, J. P. Carbone, T. G. Saunderson, M. Redies, M. Kläui, J. Ghabboun, W. Wulfhekel, S. Blügel, and Y. Mokrousov, Spin and orbital transport in rare-earth dichalcogenides: The case of eus₂, *Phys. Rev. Mater.* **6**, 074004 (2022).
- [111] A. L. R. Barbosa, L. M. Canonico, J. H. García, and T. G. Rappoport, Orbital hall effect and topology on a two-dimensional triangular lattice: From bulk to edge, *Phys. Rev. B* **110**, 085412 (2024).
- [112] S. Bhowal and S. Satpathy, Intrinsic orbital and spin hall effects in monolayer transition metal dichalcogenides, *Phys. Rev. B* **102**, 035409 (2020).
- [113] S. Bhowal and S. Satpathy, Intrinsic orbital moment and prediction of a large orbital hall effect in two-dimensional transition metal dichalcogenides, *Phys. Rev. B* **101**, 121112 (2020).
- [114] D. B. Fonseca, L. L. A. Pereira, and A. L. R. Barbosa, Orbital hall effect in mesoscopic devices, *Phys. Rev. B* **108**, 245105 (2023).
- [115] A. Veneri, T. G. Rappoport, and A. Ferreira, Extrinsic orbital hall effect: Interplay between diffusive and intrinsic transport, arXiv preprint arXiv:2408.04492 (2024).
- [116] A. Pezo, D. García Ovalle, and A. Manchon, Orbital hall physics in two-dimensional dirac materials, *Phys. Rev. B* **108**, 075427 (2023).
- [117] J. Salvador-Sánchez, L. M. Canonico, A. Pérez-Rodríguez, T. P. Cysne, Y. Baba, V. Clericò, M. Vila, D. Vaquero, J. A. Delgado-Notario, J. M. Caridad, K. Watanabe, T. Taniguchi, R. A. Molina, F. Domínguez-Adame, S. Roche, E. Diez, T. G. Rappoport, and M. Amado, Generation and control of non-local chiral currents in graphene superlattices by orbital hall effect, *Phys. Rev. Res.* **6**, 023212 (2024).
- [118] H. Sun and G. Vignale, *Theory of magnetoresistance due to edge orbital moment accumulation* (2024), arXiv:2408.02887 [cond-mat.mes-hall].
- [119] A. Faridi and R. Asgari, *Comparing the extrinsic orbital hall effect in centrosymmetric and noncentrosymmetric systems: Insights from bilayer transition metal dichalcogenides* (2025), arXiv:2501.02996 [cond-mat.mes-hall].
- [120] S. Ji, C. Quan, R. Yao, J. Yang, and X. Li, Reversal of orbital hall conductivity and emergence of tunable topological quantum states in orbital hall insulators, *Phys. Rev. B* **109**, 155407 (2024).
- [121] S. Ji, R. Yao, C. Quan, Y. Wang, J. Yang, and X. Li, Observing topological phase transition in ferromagnetic transition metal dichalcogenides, *Phys. Rev. B* **108**, 224422 (2023).
- [122] X. Mu, Y. Pan, and J. Zhou, Pure bulk orbital and spin photocurrent in two-dimensional ferroelectric materials, npj Computational Materials **7**, 10.1038/s41524-021-00531-7 (2021).
- [123] T. P. Cysne, R. B. Muniz, and T. G. Rappoport, Transport of orbital currents in systems with strong intervalley coupling: The case of Kekulé distorted graphene, *SciPost Phys. Core* **7**, 046 (2024).
- [124] T. P. Cysne, W. J. M. Kort-Kamp, and T. G. Rappoport, Controlling the orbital hall effect in gapped bilayer graphene in the terahertz regime, *Phys. Rev. Res.* **6**, 023271 (2024).
- [125] T. P. Cysne, M. Costa, M. B. Nardelli, R. B. Muniz, and T. G. Rappoport, Ultrathin films of black phosphorus as suitable platforms for unambiguous observation of the orbital hall effect, *Phys. Rev. B* **108**, 165415 (2023).
- [126] H. Liu and D. Culcer, Dominance of extrinsic scattering mechanisms in the orbital hall effect: Graphene, transition metal dichalcogenides, and topological antiferromagnets, *Phys. Rev. Lett.* **132**, 186302 (2024).
- [127] Z. Chen, R. Li, Y. Bai, N. Mao, M. Zeer, D. Go, Y. Dai, B. Huang, Y. Mokrousov, and C. Niu, Topology-engineered orbital hall effect in two-dimensional ferromagnets, *Nano Letters* **24**, 4826 (2024), pMID: 38619844, <https://doi.org/10.1021/acs.nanolett.3c05129>.
- [128] R. Li, X. Zou, Z. Chen, X. Feng, B. Huang, Y. Dai, and C. Niu, Floquet engineering of the orbital hall effect and valleytronics in two-dimensional topological magnets, *Materials Horizons* **11**, 3819–3824 (2024).
- [129] F. Reis, G. Li, L. Dudy, M. Bauernfeind, S. Glass, W. Hanke, R. Thomale, J. Schäfer, and R. Claessen, Bismuthene on a sic substrate: A candidate for a high-temperature quantum spin hall material, *Science* **357**, 287–290 (2017).
- [130] G. Li, W. Hanke, E. M. Hankiewicz, F. Reis, J. Schäfer, R. Claessen, C. Wu, and R. Thomale, Theoretical paradigm for the quantum spin hall effect at high temperatures, *Phys. Rev. B* **98**, 165146 (2018).
- [131] G.-B. Liu, W.-Y. Shan, Y. Yao, W. Yao, and D. Xiao, Three-band tight-binding model for monolayers of group-vib transition metal dichalcogenides, *Phys. Rev. B* **88**, 085433 (2013).
- [132] Y. Hu, H. Gao, and W. Ren, Ferroelectric polarization controlled orbital hall conductivity in a higher-order topological insulator: *d1t*-phase monolayer mo₂, *Phys. Rev. B* **110**, 054106 (2024).
- [133] R. Arouca, T. Nag, and A. M. Black-Schaffer, Mixed higher-order topology, and nodal and nodeless flat band

- topological phases in a superconducting multiorbital model, *Phys. Rev. B* **110**, 064520 (2024).
- [134] B. Göbel and I. Mertig, Orbital hall effect accompanying quantum hall effect: Landau levels cause orbital polarized edge currents, *Phys. Rev. Lett.* **133**, 146301 (2024).
- [135] D. Xiao, W. Yao, and Q. Niu, Valley-contrasting physics in graphene: Magnetic moment and topological transport, *Phys. Rev. Lett.* **99**, 236809 (2007).
- [136] S. Roche, S. R. Power, B. K. Nikolić, J. H. García, and A.-P. Jauho, Have mysterious topological valley currents been observed in graphene superlattices?, *Journal of Physics: Materials* **5**, 021001 (2022).
- [137] J. Lee, K. F. Mak, and J. Shan, Electrical control of the valley hall effect in bilayer mos2 transistors, *Nature Nanotechnology* **11**, 421–425 (2016).
- [138] S. Wu, J. S. Ross, G.-B. Liu, G. Aivazian, A. Jones, Z. Fei, W. Zhu, D. Xiao, W. Yao, D. Cobden, and X. Xu, Electrical tuning of valley magnetic moment through symmetry control in bilayer mos2, *Nature Physics* **9**, 149–153 (2013).
- [139] Z. Wu, B. T. Zhou, X. Cai, P. Cheung, G.-B. Liu, M. Huang, J. Lin, T. Han, L. An, Y. Wang, S. Xu, G. Long, C. Cheng, K. T. Law, F. Zhang, and N. Wang, Intrinsic valley hall transport in atomically thin mos2, *Nature Communications* **10**, 10.1038/s41467-019-08629-9 (2019).
- [140] M. Offidani, M. Milletari, R. Raimondi, and A. Ferreira, Optimal charge-to-spin conversion in graphene on transition-metal dichalcogenides, *Phys. Rev. Lett.* **119**, 196801 (2017).
- [141] M. Rodriguez-Vega, G. Schwiete, J. Sinova, and E. Rossi, Giant edelstein effect in topological-insulator-graphene heterostructures, *Phys. Rev. B* **96**, 235419 (2017).
- [142] D. MacNeill, G. M. Stiehl, M. H. D. Guimaraes, R. A. Buhrman, J. Park, and D. C. Ralph, Control of spin-orbit torques through crystal symmetry in wte2/ferromagnet bilayers, *Nature Physics* **13**, 300–305 (2016).
- [143] G. M. Stiehl, D. MacNeill, N. Sivadas, I. El Baggari, M. H. D. Guimarães, N. D. Reynolds, L. F. Kourkoutis, C. J. Fennie, R. A. Buhrman, and D. C. Ralph, Current-induced torques with dresselhaus symmetry due to resistance anisotropy in 2d materials, *ACS Nano* **13**, 2599 (2019), <https://doi.org/10.1021/acsnano.8b09663>.
- [144] H. Xu, J. Zhou, H. Wang, and J. Li, Light-induced static magnetization: Nonlinear edelstein effect, *Phys. Rev. B* **103**, 205417 (2021).
- [145] X.-G. Ye, P.-F. Zhu, W.-Z. Xu, T.-Y. Zhao, and Z.-M. Liao, Nonlinear spin and orbital edelstein effect in WTe₂, *Phys. Rev. B* **110**, L201407 (2024).
- [146] D. Li, X.-Y. Liu, Z.-C. Pan, A.-Q. Wang, J. Zhang, P. Yu, and Z.-M. Liao, Room-temperature van der waals magnetoresistive memories with data writing by orbital current in the weyl semimetal TaIrTe₄, *Phys. Rev. B* **110**, 035423 (2024).
- [147] C. Xiao, H. Liu, J. Zhao, S. A. Yang, and Q. Niu, Thermoelectric generation of orbital magnetization in metals, *Phys. Rev. B* **103**, 045401 (2021).
- [148] I. Baek, S. Han, S. Cheon, and H.-W. Lee, Nonlinear orbital and spin edelstein effect in centrosymmetric metals, *npj Spintronics* **2**, 10.1038/s44306-024-00041-4 (2024).
- [149] R. B. Atencia, D. P. Arovas, and D. Culcer, Intrinsic torque on the orbital angular momentum in an electric field, *Phys. Rev. B* **110**, 035427 (2024).
- [150] L. M. Canonico, J. H. García, and S. Roche, Spin-orbit torque emerging from orbital textures in centrosymmetric materials (2023), [arXiv:2307.14673 \[cond-mat.mes-hall\]](https://arxiv.org/abs/2307.14673).
- [151] Y. Liu and Q. Shao, Two-dimensional materials for energy-efficient spin-orbit torque devices, *ACS Nano* **14**, 9389 (2020), PMID: 32692151, <https://doi.org/10.1021/acsnano.0c04403>.
- [152] W. Tang, H. Liu, Z. Li, A. Pan, and Y. Zeng, Spin-orbit torque in van der waals-layered materials and heterostructures, *Advanced Science* **8**, 10.1002/advs.202100847 (2021).
- [153] Y. Liu, Y. Xu, A. Fert, H.-Y. Jaffres, S. Eimer, T. Nie, X. Zhang, and W. Zhao, Efficient terahertz generation from copt-based terahertz emitters via orbital-to-charge conversion, *arXiv preprint arXiv:2402.09228* (2024).
- [154] J. Kim, J. Uzuhashi, M. Horio, T. Senoo, D. Go, D. Jo, T. Sumi, T. Wada, I. Matsuda, T. Ohkubo, S. Mitani, H.-W. Lee, and Y. Otani, Oxide layer dependent orbital torque efficiency in ferromagnet/cu/oxide heterostructures, *Phys. Rev. Mater.* **7**, L111401 (2023).
- [155] D. Go, D. Jo, T. Gao, K. Ando, S. Blügel, H.-W. Lee, and Y. Mokrousov, Orbital rashba effect in a surface-oxidized cu film, *Phys. Rev. B* **103**, L121113 (2021).
- [156] J. C. Idrobo, J. Ruzs, G. Datt, D. Jo, S. Alikhah, D. Muradas, U. Noumbe, M. V. Kamalakar, and P. M. Oppeneer, Direct observation of nanometer-scale orbital angular momentum accumulation, *arXiv preprint arXiv:2403.09269* (2024).
- [157] S. Han, H.-W. Lee, and K.-W. Kim, Orbital dynamics in centrosymmetric systems, *Phys. Rev. Lett.* **128**, 176601 (2022).
- [158] J. Sohn, J. M. Lee, and H.-W. Lee, Dyakonov-perel-like orbital and spin relaxations in centrosymmetric systems, *Phys. Rev. Lett.* **132**, 246301 (2024).
- [159] M. Rang and P. J. Kelly, Orbital relaxation length from first-principles scattering calculations, *Phys. Rev. B* **109**, 214427 (2024).
- [160] V. V. Kabanov and A. V. Shumilin, Impact of the impurity symmetry on orbital momentum relaxation and orbital hall effect studied by the quantum boltzmann equation, *Phys. Rev. B* **110**, 235161 (2024).
- [161] P. Tang and G. E. W. Bauer, Role of disorder in the intrinsic orbital hall effect, *Phys. Rev. Lett.* **133**, 186302 (2024).
- [162] G. Zhu, S. A. Yang, C. Fang, W. M. Liu, and Y. Yao, Theory of orbital magnetization in disordered systems, *Phys. Rev. B* **86**, 214415 (2012).
- [163] J. Rou, C. Şahin, J. Ma, and D. A. Pesin, Kinetic orbital moments and nonlocal transport in disordered metals with nontrivial band geometry, *Phys. Rev. B* **96**, 035120 (2017).